Influence of pore-scale disorder on viscous fingering during drainage

R. Toussaint[1,3], G. Løvoll[1], Y. Méheust[2], K. J. Måløy[1] and J. Schmittbuhl[3]

[1] *Department of Physics, University of Oslo, POBox 1048 Blindern, N-0316 Oslo, Norway*

[2] *Department of Physics, NTNU Trondheim, N-7491 Trondheim, Norway*

[3] *Institut de Physique du Globe, UMR 7516, 5 rue René Descartes, 67084 Strasbourg, France*

PACS. 47.20.Gv – Viscous instability.
PACS. 47.54.+r – Pattern selection; pattern formation.
PACS. 47.55.Mh – Flows through porous media.

Abstract. – We study viscous fingering during drainage experiments in linear Hele-Shaw cells filled with a random porous medium. The central zone of the cell is found to be statistically more occupied than the average, and to have a lateral width of 40% of the system width, irrespectively of the capillary number Ca. A crossover length $w_f \propto Ca^{-1}$ separates lower scales where the invader's fractal dimension $D \simeq 1.83$ is identical to capillary fingering, and larger scales where the dimension is found to be $D \simeq 1.53$. The lateral width and the large scale dimension are lower than the results for Diffusion Limited Aggregation, but can be explained in terms of Dielectric Breakdown Model. Indeed, we show that when averaging over the quenched disorder in capillary thresholds, an effective law $v \propto (\nabla P)^2$ relates the average interface growth rate and the local pressure gradient.

Viscous fingering instabilities in immiscible two-fluid flows in porous materials have been intensely studied over the past 50 years [1], both because of their important role in oil recovery processes, and as a paradigm of simple pattern forming system. Their dynamics is controlled by the interplay between viscous, capillary and gravity forces. The ratio of viscous forces to the capillary ones at pore scale is quantified by the capillary number $Ca = \mu v_f a^2/(\gamma\kappa)$, where a is the characteristic pore size, v_f is the filtration velocity, γ the interfacial tension, κ the permeability of the cell, and μ the viscosity of the displaced fluid, supposed here much larger than the viscosity of the invading one.

There is a strong analogy between viscous fingering in porous media and Diffusion Limited Aggregation (DLA), as was first pointed out by Paterson [2]. Indeed, both processes of DLA and viscous fingering in empty Hele-Shaw cells belong to the family of Laplacian Growth Models, i.e. obey the Laplacian growth equation $\nabla^2 P = 0$, with an interfacial growth rate $v \propto -\nabla P$, where P is the diffusing field, i.e. the probability density of random walkers in DLA, or the pressure in viscous fingering. Despite differences as respectively a stochastic and deterministic growth, and boundary conditions as respectively $P = 0$ or $P = -\gamma/r$ with r the interfacial curvature, it is admitted that these processes belong to the same universality class

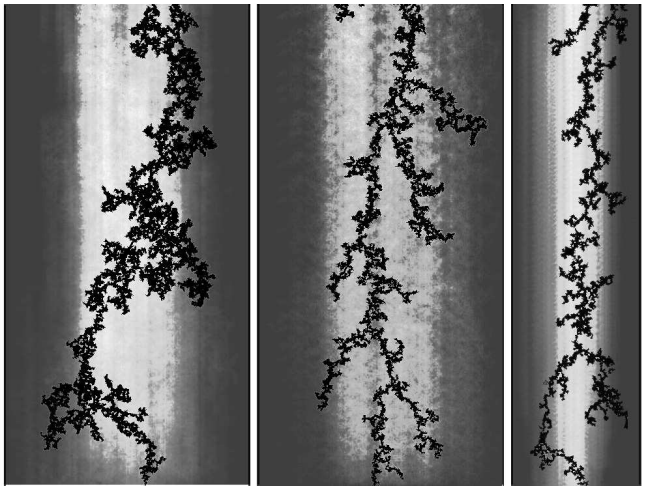

Fig. 1 – *Invasion clusters on thresholded images at capillary numbers* Ca = 0.06 **(a)** *and* 0.22 **(b,c)**, *for* $W/a = 210$ **(a,b)***and* 110 **(c)**, *with displayed system lateral boundaries. The superimposed gray map shows the occupancy probability* $\pi(x, z)$ *of the invader, in a moving reference frame attached to the most advanced invasion tip and to the lateral boundaries.*

[2–4]. In radial geometry these processes lead to fractal structures of dimensions $D = 1.70 \pm 0.03$ [5], 1.713 ± 0.0003 [6], and 1.7 [4] respectively in viscous fingering in empty Hele-Shaw cells, DLA, and numerical solutions of deterministic Laplacian growth. The two numerical models have been reexplored recently using stochastic conformal mapping theory [3, 4, 6]. However, in Hele-Shaw cells filled with disordered porous materials similar to the one used here, a lower fractal dimension $D = 1.58 \pm 0.09$ has been measured [7].

In straight channels, DLA gives rise to fractal structures of dimension 1.71, occupying on average a lateral fraction $\lambda = 0.62$ of the system width W [8]. Viscous fingering in empty Hele-Shaw cell converge towards the Saffman Taylor (ST) solution [9], with a uniformly propagating fingerlike interface covering a fraction $\lambda = 0.5$ of the system width at large capillary numbers [9, 10], selected by the interfacial tension [11].

For straight channels with a disordered porous medium, viscous fingering with a non-wetting invader leads to a branched structure that depends on Ca , on the observation scale and on the system size (Fig. 1). Løvoll et al [12] recently investigated the growth activity of the invading fluid in such systems, and showed that up to statistical fluctuations, the characteristic number of pores invaded at a given longitudinal distance behind the most advanced tip is a stationary quantity (denoted $n(z)$ in [12]). In this Letter, we extend the experimental characterization of the probability occupancy function of the invader, and obtain a universal invasion probability function $\pi(x, z)$, which in reduced coordinates is independent of capillary numbers and system sizes. This function represents the fraction of invaded pores in the reference frame of the stationary process. To our knowledge, this is the first experimental attempt to reach such a quantity, and represents a technical challenge due to the required high number of experiments, and the need for the development of good automation techniques for image data processing. We also characterize in details the fractal geometry of the invasion structure, and its different regimes at different scales. In this Letter, we also provide a theoretical argument which takes into account the influence of the disorder in the capillary

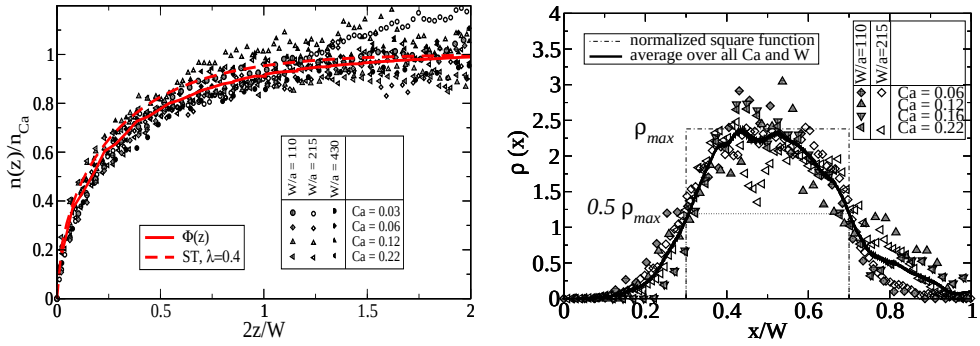

Fig. 2 – *Scaled invader's density, after projections along directions parallel or perpendicular to the average flux, as function of reduced coordinates scaled by the system width* W*. (a): Scaled density* $n(z)/n_{Ca}$ *as function of* $2z/W$*, scaled longitudinal distance to the most advanced tip, for three system sizes and four capillary numbers. The lines are the experimental averages, and the theoretical Saffman Taylor solution for a single finger occupying a lateral fraction* $\lambda = 0.4$ *of the system. (b): Normalized density as function of the scaled lateral coordinate,* $\rho(x)$*, with half-maximum reached over a width* $0.4W$

thresholds along the invasion front, and we establish that if indeed at high capillary number, the process is well described by DLA as often suggested [2], there is also at intermediate Ca a regime where the flow in *random* porous media is better described by another Laplacian model, namely a Dielectric Breakdown Model (DBM) with $\eta = 2$ – the interfacial growth rate is $v \propto (\nabla P)^\eta$ in DBM, $\eta = 1$ corresponding to DLA –. This theoretical argument leads to estimates of the fractal dimensions of the invader, and of the lateral fraction λ characteristizing the geometry of the invasion probability function, which are compatible with the experimental results.

In the experiments, linear Hele-Shaw cells of thickness $a = 1$mm were filled at 38% with a monolayer of randomly located immobile glass beads of diameter a, between which air displaces a solution of 90% glycerol - 10% water of much larger viscosity $\mu = 0.165$ Pa·s, wetting the beads and walls of the cell, i.e. in drainage conditions (experimental technique similar to [12]). The interfacial tension and the permeability of the cell are respectively $\gamma = 0.064$ N·m^{-1} and $\kappa = 0.00166 \pm 0.00017$ mm^2. We investigate regimes ranging from capillary to viscous fingering ($0.01 < Ca < 0.5$), in cells with impermeable lateral walls and dimensions $W \times L \times a$, with widths perpendicularly to the flow direction $W/a = 110$, 215 and 430, and a length $L/a = 840$. The cell is set horizontally, so that gravity is irrelevant. A constant filtration rate of water-glycerol is ensured by a controlled gravity-driven pump.

Pictures of the flow pattern are taken from the top, and treated to extract the invading air cluster (with pixels of size $0.55a$), as the black clusters in Fig. 1. In ref. [12], we have shown that the invasion process is stationary, up to fluctuations arising from the disorder in pore geometries. To extract the underlying average stationary behavior, all quantities are then analyzed in the reference frame (x, z) attached to the lateral boundaries at $x = 0$ and $x = W$, and to the foremost propagating tip at $z = 0$, z pointing against the flow direction (this tip indeed propagates at a roughly constant speed v_{tip} [12]). Average quantities at any position (x, z) of the tip related frame, are defined using all stages and points of the invasion process, excluding regions closer than $W/2$ from the inlet or outlet, to avoid finite size effects.

The average occupancy map $\pi(x, z)$ is defined as follows: for each time (or each picture), we

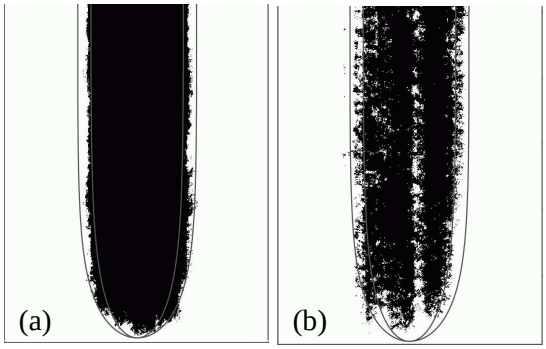

Fig. 3 – *(a) Average occupation density map of the invader thresholded at half-maximum, for a system size W/a=215, in the reference frame attached to the tip position, at* $Ca = 0.06$ *(a) and* 0.22 *(b), compared to ST curves for* $\lambda = 0.35$ *and* 0.45.

assign the value 1 to the coordinate (x, z) if air is present there, 0 otherwise. $\pi(x, z)$ obtained as the time average of such occupancy function, is displayed as graymap in Fig. 1. This definition would coincide, in the limit of large systems, with the mean occupancy introduced for DLA by Arneodo et al. [8,13]. Next we compute the average number of occupied pores per unit length at a distance z behind the tip, $n(z)$, which is related to π as $n(z) = (1/a^2) \int_0^W \pi(x, z)\, dx$. We show in Fig. 2 (a), a data collapse for all experiments, at different capillary numbers Ca and three system widths W, of $n(z)/n_{Ca} = \Phi(2z/W)$, where $n_{Ca} = (W/a^2)v_f/v_{tip}$ [12]. The underlying scaling function Φ is a function increasing from 0 at $z = 0$ towards 1 at $z = +\infty$, as granted by conservation of the displaced fluid for a statistically stationary process [12]. Φ is evaluated in Fig. 2 (a) as an average over all experiments and sizes.

We also characterize the lateral structure of the invader in the frozen zone, $z > W$, where less than 10% of the invasion activity takes place since $\Phi(2) > 0.9$. We define over this zone a distribution in reduced coordinates $\rho(x) = [W/(a^2\, n_{Ca})]\, \pi(x, \infty) = (v_{\rm tip}/v_{\rm f})\, \pi(x, \infty)$, so that $\int_0^W \rho(x)dx/W \simeq 1$. This quantity, presented in Fig. 2(b) for an average over five experiments at capillary numbers $Ca = 0.06$ and 0.22 for $W/a = 215$, and for four experiments with $0.06 < Ca < 0.22$ for $W/a = 110$, seems also reasonably independent of system size and capillary number, as is $n(z)/n_{Ca}$ – Fig. 2(a). We notice a certain dispersion around the average, but no systematic trend over size or capillary number. An interesting geometrical characteristic of this underlying lateral occupation density is the fraction λ of the system, occupied by the invader at saturation, which is evaluated as in [8]: $\lambda = 1/\rho_{max}$, or alternatively $\lambda = (x^+ - x^-)/W$, where $\rho(x^+) = \rho(x^-) = \rho_{max}/2$. Both definitions, for a regular function $\rho(x)$ determined by averaging over capillary numbers and sizes, lead to $\lambda \simeq 0.4 \pm 0.02$ as shown in Fig. 2(b): this is significantly smaller than the off-lattice DLA result $\lambda = 0.62$ [8,14].

The 2D occupancy map $\pi(x, z)$ itself, displayed as graymap in Fig. 1, has a maximum $\pi_{\rm max} = \rho_{\rm max} v_f/v_{\rm tip}$, along a line at $(x = W/2, z > W)$. Similarly to Arneodo's procedure [8], we determine the support of $\pi > \pi_{max}/2$, displayed in Fig. 3(a) and (b), which corresponds to the most often occupied region. Within the noise error, the shape of this region resembles the theoretical ST curve corresponding to $\lambda = 0.4 \pm 0.05$ [9] (gray lines in Fig. 3). For such a theoretical ST finger, this curve would also coincide with another observable determined in this study, namely the scaled longitudinal density of invader. As seen in Fig. 2(b), there are

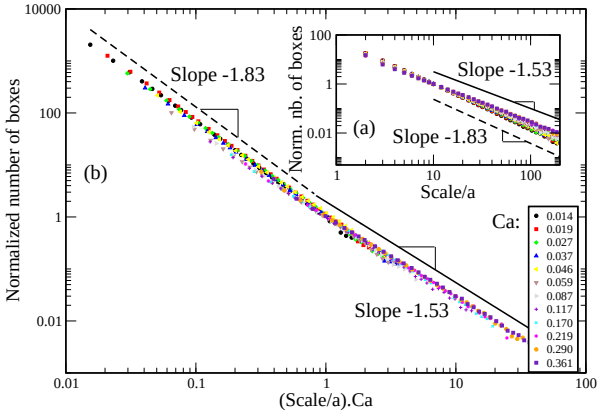

Fig. 4 – *Small and large scale fractal dimension of the invasion cluster at various capillary numbers, determined by box-counting. (a) insert: number of boxes as function of the scale. (b): Data collapse for all capillary numbers after rescaling the box size by Ca: evidence of cross over scale $w_f \sim Ca^{-1}$ separating a small scale capillary fractal dimension 1.83, and large viscous scale 1.53.*

also similarities between the two processes for this other observable, i.e. between the scaled longitudinal density $\Phi(z)$ determined for the fingering process in disordered media studied here (continuous line), and this theoretical ST curve corresponding to $\lambda = 0.4$ (dashed line). Systematic deviations from the mathematical ST solution at $\lambda = 0.4$ might nonetheless exist for these two observables, accordingly to what has been seen between the DLA envelopes and the corresponding ST solution at $\lambda = 0.62$ [14].

The mass fractal dimension of the invasion clusters is analyzed by box-counting. $N(s)$ is the number of boxes of size s to cover the invader. Fig. 4 displays a normalized distribution $N(s)/N(a/Ca)$ as function of $(s/a) \cdot Ca$ for various capillary numbers. By linear regression of this collapsed log-log data, we find that $N(s) \sim s^{-1.83 \pm 0.01}$ for small scales $s < a/Ca$, and $N(s) \sim s^{-1.53 \pm 0.02}$ for larger scales. The result can be explained by the following approximations. The distribution of pore throats sizes results in a distribution of capillary pressure thresholds P_t, $g(P_t)$, of characteristic width W_t. Consider a box of size w_f along the cluster boundary in the active zone, such that $w_f \cdot \nabla P_b = W_t$ where ∇P_b is a characteristic pressure gradient. At scales $s < w_f$, viscous pressure variations are lower than capillary threshold fluctuations, and the most likely invaded pores correspond to the lowest random thresholds, which corresponds to capillary fingering, thus leading to $D = 1.83$ (similarly to capillary fingering experiments [15], or to invasion percolation model [16]). Conversely, at larger sizes ($s > w_f$), the invasion activity is determined essentially by the spatial variations of ∇P_b. Assuming that ∇P_b scales as the imposed $\nabla P(-\infty) \propto Ca$, i.e. neglecting the geometry variations between different speeds, w_f scales as $W_t/\nabla P_b \propto a/Ca$, as confirmed by the data collapse in Fig. 4(a). Such a scaling law, $w_f/a \propto Ca^{-1}$ before saturating at large Ca, is also consistent with another experimental determination of w_f, illustrated in Fig. 9 of Ref. [12]

Eventually, we sketch a possible explanation for the width selection $\lambda = 0.4$ and the large scale fractal dimension $D = 1.53 \pm 0.02$, which are smaller than their counterparts in DLA, respectively 0.62 and 1.71. Neglecting the small scale permeability variations leads to a Laplacian pressure field in the defending fluid. The boundary condition for the pressure field is then $\nabla P(z = -\infty) = -\mu v_f/\kappa$, and $\nabla P(x = 0, W) \cdot \hat{x} = 0$ where $\hat{x}$ is the unit vector along x. The dynamics of the process is then entirely controlled by the boundary

condition along the invading fluid, i.e. by the capillary pressure drop across the meniscus in the pore neck and the pressure gradient in the invaded fluid. For a given pressure difference at pore scale between the invading air at P_0, and the pressure P_1 in the glycerol-filled pore, we decompose $P_0 - P_1 = \Delta P_v + P_c$, where ΔP_v is a viscous pressure drop in the pore neck, and the capillary pressure drop is $P_c = \gamma/r + 2\gamma/a$, where the in- and out-of-plane curvature of the interface are respectively r and $a/2$. As a meniscus progresses between neighboring beads, its curvature goes through a minimum r_m in the pore neck. The meniscus will be able to pass the neck if the pressure drop $P_0 - P_1$ exceeds the threshold $P_t = P_c(r_m)$. For the sake of simplicity, the probability distribution of the thresholds $g(P_t)$ is considered flat, between P_{min} and P_{max}, with $W_t = P_{max} - P_{min}$ and $g(P_t) = \theta(P_t - P_{min})\theta(P_{max} - P_t)/W_t$, where θ is the Heaviside function. In the pure capillary fingering limit $Ca \to 0$, the pressure field P is homogeneous in the defending fluid, and a pore is invaded when $P_0 - P$ reaches the minimum threshold along the boundary, close to P_{min}. At higher capillary number, we want to relate the invasion rate to the local capillary threshold, and to the pressure P_1 in the liquid-filled pore nearest to the interface. If $P_0 - P_1 < P_t$, the meniscus adjusts reversibly in the pore neck, and the next pore is not invaded. Conversely, if $P_0 - P_1 > P_t$, the pore will be invaded, and most of the invasion time is spent in the thinnest region of the pore neck. A characteristic interface velocity can be evaluated by the Washburn equation [17] at this point: $v \sim -(2\kappa/\mu a)(P_0 - P_1 - P_t)\theta(P_0 - P_1 - P_t)$, where the heaviside function results from a zero invasion velocity if the pore is not invaded. Hypothesizing that only the average growth rate controls the process, independently of the particular realization of random thresholds, the growth rate averaged over all possible pore neck configurations, is

$$\begin{aligned} < v > &= \int \frac{-2\kappa}{\mu a}(P_0 - P_1 - P_t)\theta(P_0 - P_1 - P_t)g(P_t)dP_t \\ &= -(\kappa/\mu a)\theta(P_0 - P_1 - P_{min}) \times \\ &\quad \{[(P_0 - P_1 - P_{min})^2/W_t]\theta[P_{max} - (P_0 - P_1)] + \\ &\quad 2[P_0 - P_1 - (P_{min} + P_{max})/2]\theta[P_0 - P_1 - P_{max}]\}. \end{aligned} \tag{1}$$

At moderate capillary numbers, such as $P_0 - P_1 < P_{max}$, if we assume that the capillary pressure drop is around $P_c = P_{min}$ when the invasion meniscus is at the entrance of the pore neck, we note that $(P_0 - P_{min} - P_1)/a = \Delta P_v/a \sim \nabla P/2$, and Eq. (1) implies that the growth rate goes as $< v >= -a\kappa/(4\mu W_t)(\nabla P)^2$. This effective quadratic relationship between the average growth rate and the local pressure gradient arises from the distribution of capillary thresholds, and means that such invasion process should be in the universality class of DBM with $\eta = 2$, rather than DLA (DBM, $\eta = 1$). Indeed, in DBM simulations in linear channels, λ is a decreasing function of η (as in related deterministic problems, as viscous fingering in shear-thinning fluids [18], or η-model [19]), and Somfai et al. [14] report $\lambda \simeq 0.62$ and 0.5 for respectively $\eta = 1$ and 1.5, so that the observed $\lambda = 0.4$ is consistent with $\eta = 2$. The fractal dimension of DBM is also a decreasing function of η, and $\eta = 2$ corresponds $D = 1.4 \pm 0.1$ [20], which is close to the observed $D = 1.53 \pm 0.02$ in our experiments.

Note that at high capillary numbers such that locally $P_0 - P_1 \gg P_{max}$, the threshold fluctuations are not felt by the interface, and Eq. (1) leads to $< v_{inv} >= -(\kappa/\mu)\nabla P$, which would correspond to a classic DLA process. We have checked by numerically solving the Laplace equation with the experimental clusters as boundaries that all experiments performed here were at moderate enough capillary number to have $P_0 - P_1 < P_{max}$ all along the boundary [12], i.e. the quadratic law $< v >= -a\kappa/(4\mu W_t)(\nabla P)^2$ is expected to hold.

Even at moderate Ca, deviations from the DBM model with $\eta = 2$ could be observed for significantly non-flat distribution of the capillary thresholds in the random porous medium,

for which Eq.(1) would lead to a more complicated dependence of the growth rate v on ∇P, reflecting the details of this distribution, and not simply a power-law effective relationship. It would be interesting in future work to explore numerically and experimentally the detailed effect of non-flat capillary threshold distributions on the selected fractal dimension, average width occupied in the system, and total displaced mass $n_{Ca}(Ca)$ (reported in [12] for the present work), to extract the influence of the disorder on the best capillary number to select in order to maximize the efficiency of the extraction process.

We acknowledge with pleasure fruitful discussions with E. G. Flekkøy, A. Lindner, A. Hansen and E. Somfai, and support from the PICS program granted by NFR and CNRS.

REFERENCES

[1] D. Bensimon, L. P. Kadanoff, S. Liang, B. I. Shraiman, and C. Tang. Viscous flows in two dimensions. *Rev. Mod. Phys.*, 58:977, 1986.

[2] L. Paterson. Diffusion-limited aggregation and two-fluid displacements in porous media. *Phys. Rev. Lett.*, 52:1621–1624, 1984.

[3] M. G. Stepanov and L. S. Levitov. Laplacian growth with separately controlled noise and anisotropy. *Phys. Rev. E*, 63:061102, 2001.

[4] A. Levermann and I. Procaccia. Algorithm for parallel laplacian growth by iterated conformal maps. *Phys. Rev. E*, 69:031401, 2004.

[5] E. Sharon, M. G. Moore, W. D. McCormick, and H. L. Swinney. Coarsening of fractal viscous fingering patterns. *Phys. Rev. Lett.*, 91:205504, 2003.

[6] B. D. Davidovitch, A. Levermann, and I. Procaccia. Convergent calculation of the asymptotic dimension of dla: scaling and renormalization of small clusters. *Phys. Rev. E*, 62:R5919, 2000.

[7] E. L. Hinrichsen, K. J. Måløy, J. Feder, and T. Jøssang. Self-similarity and structure of dla and viscous fingering clusters. *J. Phys. A*, 22:L271–L277, 1989.

[8] A. Arneodo, J. Elezgaray, M. Tabard, and F. Tallet. Statistical analysis of off-lattice diffusion-limited aggregates in channel and sector geometries. *Phys. Rev. E*, 53:6200, 1996.

[9] P. G. Saffman and G Taylor. The penetration of a fluid into a porous medium or hele-shaw cell containing a more viscous liquid. *Proc. Soc. London*, Ser. A 245:312–329, 1958.

[10] P. Tabeling, G. Zocchi, and A. Libchaber. An experimental study of the saffman-taylor instability. *J. Fluid Mech.*, 177:67, 1987.

[11] J. W. McLean and P. G. Saffman. The effect of surface tension on the shape of fingers in a hele-shaw cell. *J. Fluid Mech.*, 102:445, 1981.

[12] G. Løvoll, Y. Méheust, R. Toussaint, J. Schmittbuhl, and K. J. Måløy. Growth activity during fingering in a porous hele-shaw cell. *Phys. Rev. E*, 70:026301, 2004.

[13] A. Arneodo, Y. Couder, G. Grasseau, V. Hakim, and M. Rabaud. Uncovering the analytical saffman-taylor finger in unstable viscous fingering and diffusion-limited aggregation. *Phys. Rev. Lett.*, 63:984, 1989.

[14] E. Somfai and R. C. Ball. Diffusion-limited aggregation in channel geometry. *Phys. Rev. E*, 68:020401, 2003.

[15] R. Lenormand and C. Zarcone. Invasion percolation in an etched network: measurement of a fractal dimension. *Physical Review Letters*, 54(20):2226–2229, 1985.

[16] R. Chandler, J. Koplik, K. Lerman, and J. F. Willemsen. Capillary displacement and percolation in porous media. *Journal Fluid Mechanics*, 119:249–267, 1982.

[17] E. W. Washburn. The dynamics of capillary flow. *Phys. Rev.*, 17:273, 1921.

[18] A. Lindner, D. Bonn, E. Corvera Poiré, M. Ben Amar, and J. Meunier. Viscous fingering in non-newtonian fluids. *J. Fluid Mech.*, 469:237, 2002.

[19] M. Ben Amar. Viscous fingering: a singularity in laplacian growth models. *Phys. Rev. E*, 51:R3819, 1995.

[20] J. Mathiesen and M. H. Jensen. Tip splittings and phase transitions in the dielectric breakdown model: Mapping to the diffusion-limited aggregation model. *Phys. Rev. Lett.*, 88:235505, 2002.